Solar Phys (2014) 289:1239–1256
DOI 10.1007/s11207-013-0405-6

Imaging Observations of X-Ray Quasi-periodic Oscillations at 3 – 6 keV in the 26 December 2002 Solar Flare

Zongjun Ning

Received: 13 November 2012 / Accepted: 27 August 2013 / Published online: 2 October 2013

Abstract Quasi-periodic oscillations in soft X-rays (SXR) are not well known due to the instrument limitations, especially the absence of imaging observations of SXR oscillations. We explore the quasi-periodic oscillations of SXR at 3 – 6 keV in a solar flare observed by the *Reuven Ramaty High Energy Solar Spectroscopic Imager* (RHESSI) on 26 December 2002. This was a B8.1 class event and showed three X-ray sources (S_1, S_2, and S_3) at 3 – 6 keV and two sources (S_1 and S_2) at 12 – 25 keV. The light curves of the total fluxes display a two-minute oscillation at 3 – 6 keV, but not in the energy bands above 8 keV. To investigate imaging observations of the oscillations, we prepared CLEAN images at seven energy bands between 3 keV and 20 keV with an eight-second integration. The light curves of three sources were analyzed after integrating the flux of each source region. We used the Fourier method to decompose each source light curve into rapidly varying and slowly varying components. The rapidly varying components show seven individual peaks which are well fitted with a sine function. Then we used the wavelet method to analyze the periods in the rapidly varying component of each source. The results show that three sources display damped quasi-periodic oscillations with a similar two-minute period. The damped oscillations timescale varies between 2.5 to 6 minutes. Source S_1 oscillates with the same phase as S_3, but is almost in anti-phase with S_2. Analyzing the flaring images in more detail, we found that these oscillation peaks are well consistent with the appearance of S_3, which seems to split from or merge with S_2 with a period of two minutes. The flare images with a high cadence of one second at 3 – 6 keV show that source S_3 appears with a rapid period of 25 seconds. The two-minute oscillation shows the highest spectral power. Source S_3 seems to shift its position along the flare loop with a mean speed of 130 km s^{-1}, which is of the same order as the local sound speed. This connection between the oscillation peaks and emission enhancement appears to be an observational constraint on the emission mechanism at 3 – 6 keV.

Z. Ning (✉)
Key Laboratory of Dark Matter and Space Astronomy, Purple Mountain Observatory, Nanjing 210008, China
e-mail: ningzongjun@pmo.ac.cn

Z. Ning
Key Laboratory of Solar Activity, National Astronomical Observatories, Beijing 100012, China

Keywords Flares · X-ray bursts, soft

1. Introduction

Solar flaring emissions are observed to display quasi-periodic oscillations in a broad frequency range from radio through visible and extreme-ultraviolet (EUV) light to X-rays (Isliker and Benz, 1994; Kliem, Karlický, and Benz, 2000; Asai *et al.*, 2001; Melnikov *et al.*, 2005; Foullon *et al.*, 2005; Ning *et al.* 2005, 2007; Nakariakov *et al.*, 2006; Ofman and Sui, 2006; Li and Gan, 2008; Zimovets and Struminsky, 2009; Nakariakov and Melnikov, 2009; Sych *et al.*, 2009; Tan *et al.*, 2010; Kupriyanova *et al.*, 2010; Su, Shen, and Liu, 2012; Su *et al.*, 2012). Typical periods of these oscillations range from a few milliseconds to several minutes. Mangeney and Pick (1989) and Zhao, Mangeney, and Pick (1991) reported quasi-periodicity ranges of between one and six seconds in Type III radio bursts using Fourier transformation. They concluded that this kind of quasi-periodicity occurs because of the quasi-periodic process in solar flares. Using radio dynamic spectra in the frequency range of 100 – 500 MHz, Aschwanden, Benz, and Montello (1994) statistically studied the quasi-periodicity of Type III bursts in 260 solar flares and found a mean quasi-period of 2.0 ± 1.2 seconds. More recently, Ning *et al.* (2005) studied the quasi-periodicity of reverse Type III bursts in the frequency range of 4.5 – 7.5 GHz in 22 solar flares and found a mean period of about 2.0 ± 0.6 seconds. However, Isliker and Benz (1994) did not find any hint of a quasi-periodic behavior for Type III bursts. At EUV wavelengths, the quasi-periodic oscillations are often observed in coronal loops (*e.g.* Aschwanden *et al.*, 1997; Nakariakov *et al.*, 1999; De Moortel *et al.*, 2002; Wang *et al.*, 2002; Kliem *et al.*, 2002; Su, Shen, and Liu, 2012; Su *et al.*, 2012). These oscillations have long periods of tens of minutes and are generally thought to be related to solar-flare eruptions (Ofman and Wang, 2002; Wang *et al.*, 2003).

Hard X-ray time profiles obtained from earlier observations often did not show periodic behaviors in flare light curves due to photon-noise limitation. More sensitive instruments such as the *Burst and Transient Source Experiment* (BATSE) onboard the *Compton Gamma Ray Observatory* (CGRO) and the *Reuven Ramaty High Energy Solar Spectroscopic Imager* (RHESSI: Lin *et al.*, 2002) clearly revealed quasi-period structures on the subsecond or minute timescale at nonthermal energies (*e.g.* Hoyng, van Beek, and Brown, 1976; Lipa, 1978; Bogovalov *et al.* 1983, 1984; Svestka *et al.*, 1982; Harrison, 1987; McKenzie and Mullan, 1997; Foullon *et al.*, 2005; Dmitriev *et al.*, 2006; Zimovets and Struminsky, 2010). Aschwanden *et al.* (1995) systematically studied 640 BATSE flares with an automated pulse-detection algorithm. They found a total of 5430 individual pulses with a typical duration of 0.3 – 1.0 seconds. The modulation depth of these pulses typically varied in a range of 10 % – 50 %. RHESSI observed a few samples of HXR oscillation with quasi-periods ranging from four to ten minutes (Foullon *et al.*, 2005; Nakariakov *et al.*, 2006; Ofman and Sui, 2006; Li and Gan, 2008). A good example of the quasi-periodic oscillations observed from microwave to hard X-ray was shown by Li and Gan (2008), who studied an M2.6 flare on 22 August 2005 that displayed a damped oscillation with a period of four minutes. An oscillation with a short period of about six seconds was observed in both microwave and hard X-ray emission in the 10 November 1998 flare (Asai *et al.*, 2001). Moreover, Nakajima *et al.* (1983) reported two flares that displayed an oscillation with a quasi-period of eight seconds from microwave through hard X-ray to γ-ray emissions. Nakariakov *et al.* (2010) reported an oscillation with a period of about 40 seconds in a single X-class flare loop in high-energy γ-rays.

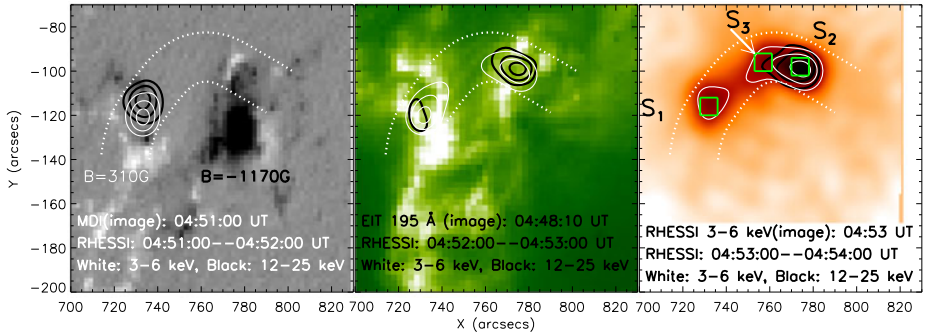

Figure 1 SOHO/MDI magnetogram at 04:51:00 UT (left), SOHO/EIT 195 Å image at 04:48:10 UT (middle) with RHESSI X-ray contours at 04:51:00 – 04:52:00 UT, RHESSI 3 – 6 keV images at 04:53:00 UT with its contours (right): all on 26 December 2002. The two dotted lines outline the flaring loop to cover the three sources S_1, S_2, and S_3. The contour levels are set at 60 %, 70 %, and 90 % for 3 – 6 keV (white) and 12 – 25 keV (black).

Understanding the quasi-periodic oscillation during the flare eruption is still an open question. The fundamental physical processes of these oscillations in solar flares are thought to be relevant to magnetic reconnection, MHD waves, particle acceleration, thermodynamics, and other kinetic effects. Nakariakov *et al.* (1999) suggested that the quasi-periodic oscillations with a period of several minutes could provide remote diagnostics of solar plasma. Aschwanden *et al.* (1998) found that the shortest timescale is proportional to the flare-loop radius, while it is anti-correlated with the trapped electron density in the loops detected from the SXRs, indicating that the quasi-periodic oscillations are observational evidence of a periodic pumping of nonthermal electrons in a flaring loop, usually modulated by certain waves with varying periods. The oscillations in the nonthermal emissions such as microwaves, HXRs, and γ-rays are thought to be evidence of periodic acceleration in solar flares. It seems that the acceleration process is modulated by MHD waves to display various periods from the observations (Foullon *et al.*, 2005; Nakariakov *et al.*, 2006; Nakariakov, 2007; Nakariakov and Melnikov, 2009).

Quasi-periodic oscillations in HXR (*i.e.* above 20 keV) emission are widely reported and studied (Nakajima *et al.*, 1983; Aschwanden *et al.*, 1998; Asai *et al.*, 2001; Nakariakov *et al.*, 2006; Ofman and Sui, 2006; Li and Gan, 2008). The oscillatory behavior in low-energy X-ray emission has previously been studied in some samples of solar flares (*e.g.* Svestka *et al.*, 1982; Harrison, 1987; McKenzie and Mullan, 1997; Foullon *et al.*, 2005; Dmitriev *et al.*, 2006; Zimovets and Struminsky, 2010). However, its fundamental mechanism is not well understood yet and needs more observational information from samples with oscillation behavior in low-energy X-rays. With its full-disk solar imaging possibility, wide energy coverage (3 – 17 000 keV), and high sensitivity, RHESSI provides unprecedented capabilities for investigating quasi-periodic oscillations at 3 – 6 keV X-ray emissions with a high temporal resolution. Here, we analyze the imaging observations of a quasi-periodic oscillation at 3 – 6 keV for the 26 December 2002 solar flare.

2. Observation and Measurement

The flare studied here is the B8.1 event on 26 December 2002. It started at 04:48 UT, reached its maximum at 04:52 UT, and ended at 05:04 UT from GOES SXR observations. Figure 1 shows a magnetogram from the *Michelson Doppler Image* (MDI: Scherrer *et al.*, 1995)

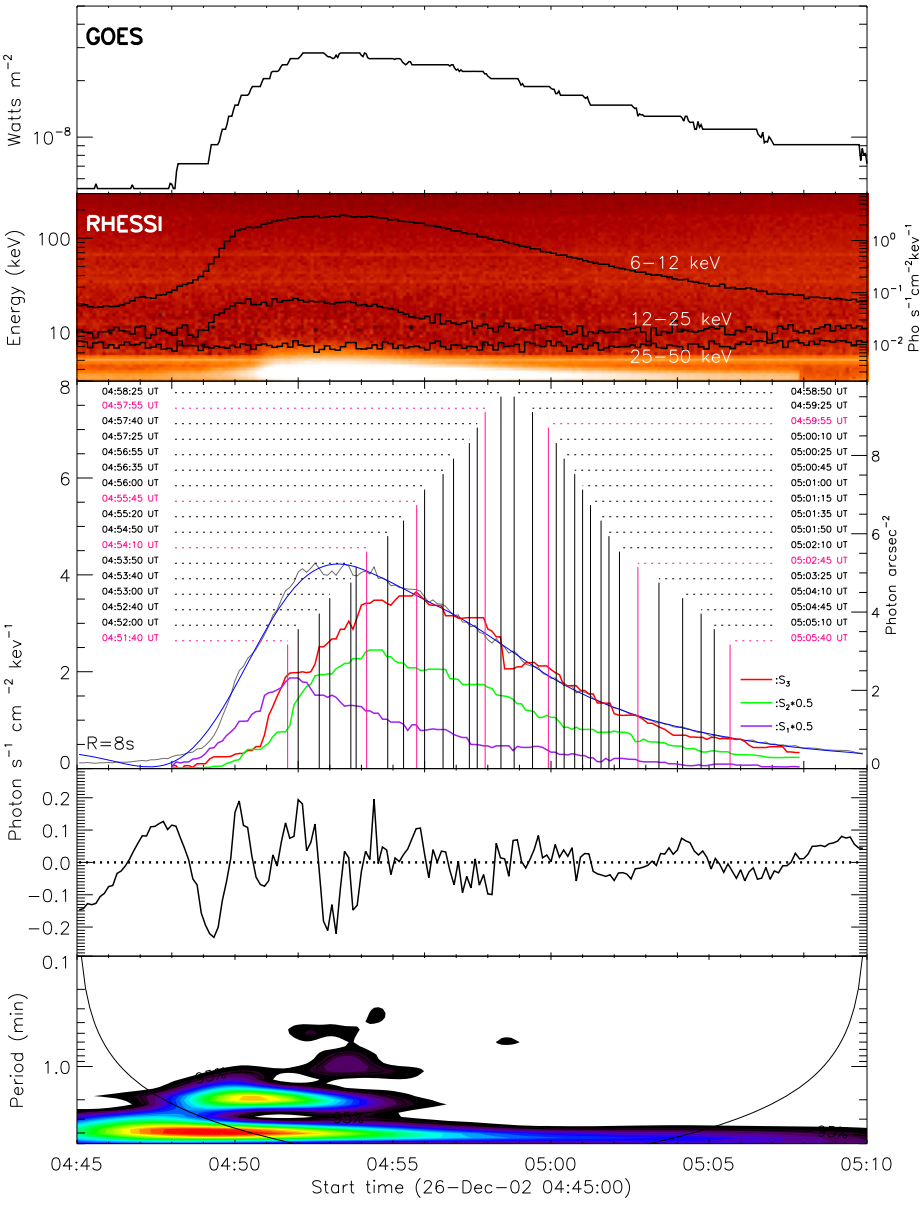

Figure 2 Temporal evolution of GOES SXR 1 – 8 Å light curve (top), RHESSI dynamic spectra at 3 – 300 keV (second), the RHESSI 3 – 6 keV light curve (third), its rapidly varying component (fourth), and wavelet spectra (bottom). The RHESSI light curves at 6 – 12 keV, 12 – 25 keV, and 25 – 50 keV are given in the second panel. Integrated fluxes of S_1 (purple), S_2 (green), and S_3 (red) are shown from 04:48 UT to 05:08 UT with an eight-second temporal resolution, and each vertical line labels the times of the peaks (pink) or subpeaks (black) on the S_3 light curves.

onboard the *Solar and Heliospheric Observatory* (SOHO: Domingo, Fleck, and Poland, 1995) at 04:51 UT (left), the *Extreme ultraviolet Imaging Telescope* (EIT: Delaboudinière

et al., 1995) 195 Å image at 04:48 UT (middle), and a RHESSI 3 – 6 keV image at 04:53 UT (right) with X-ray contours at 3 – 6 keV (white) and 12 – 25 keV (black), respectively. We constructed the RHESSI CLEAN image with a one-minute integration window. The flare displays three sources at 3 – 6 keV, marked by S_1, S_2, and S_3 in Figure 1, while there are only two sources S_1 and S_2 at 12 – 25 keV. It appears that S_1 and S_2 are two footpoint sources, while S_3 is the loop-top source. In this case, the flare loop is assumed to connect S_1 with S_2 through S_3. The two dashed lines in Figure 1 outline the flare loop that tries to cover the X-ray maximum brightness at various energy bands (at 3 – 6 keV, 6 – 12 keV, and 12 – 25 keV) and various times (from 04:50 UT to 05:05 UT). This method has been used before to sketch a flare loop from RHESSI observations (Ning, 2011; Ning and Cao, 2011). Figure 1 (left) shows that the two footpoints of this loop tend to locate the positive and negative magnetic fields. According to the standard model, solar flares usually display a single SXR source at 3 – 6 keV around the loop top, but two footpoint HXR sources (*i.e.* at 25 – 50 keV) around the footpoints (*e.g.* Masuda *et al.*, 1994). Sometimes, the solar flare displays a loop structure at 3 – 6 keV (*e.g.* Ning, 2011). It is interesting that the 26 December 2002 event displays two footpoint sources [S_1 and S_2] at an energy as low as 3 – 6 keV around the footpoints, similar to that at 12 – 25 keV, especially at 04:52 UT. Figure 1 shows that this event starts to brighten around the source S_1 initially, then S_2 gradually becomes bright, while S_1 weakens gradually. The loop top (S_3, the arrow in Figure 1 (right)) source at 3 – 6 keV appears and becomes bright simultaneously with S_1. Three green boxes show the regions of the three sources S_1, S_2, and S_3. The box positions are fixed and they are large enough (8×8 arcsec^2 here) to cover and trace the main emissions of the three sources during the flare development. On the other hand, it is possible that the sources S_1 and S_2 are not the footpoints of one large flare loop shown by the two dashed lines in Figure 1, but instead are two different subsystems of smaller flaring loops. SOHO/MDI observations show the mixed magnetic polarities in the regions S_1 and S_2. The complex structure of the flare ribbons in S_1 and S_2 is seen in the SOHO/EIT image.

2.1. Total Flux Oscillation at 3 – 6 keV

Figure 2 shows GOES (top panel) and RHESSI (second to fourth panels) observations of this event. As mentioned before, GOES SXR shows this flare as a weak B-class event, and the nonthermal emission is so faint that RHESSI HXR above 25 keV emissions are quiet. In contrast to the smooth light curves at 6 – 12 keV and 12 – 25 keV, the 3 – 6 keV emission displays several peaks on its light curve, especially around the flux maximum, shown as the thick gray line in Figure 2 (third panel). Amplitudes of these peaks have a mean value of 0.34 photons s^{-1} cm^{-2} keV^{-1}, which is four times higher than the amplitude of the pre-flare background noise (about 0.08 photons s^{-1} cm^{-2} keV^{-1}). It seems that there is a quasi-periodic oscillation among these peaks. Note here that the light curves at 3 – 6 keV, 6 – 12 keV, and 12 – 25 keV are the total fluxes from the Sun, and the temporal resolution is eight seconds. To distinguish these peaks from the background emission, we decomposed the 3 – 6 keV light curve into a rapidly varying component and a slowly varying component using the Fourier method. First, we used the fast Fourier transform to calculate the power spectrum of the light curves. Then we split the power spectrum into a lower- and higher-frequency domain. Finally, we applied the inverse fast Fourier transform to the two parts of the power spectrum to obtain the slowly varying (background) and rapidly varying (quasi-periodic peak) components (Jin and Ding, 2007). The threshold timescale between the two components was arbitrarily chosen to be 240 seconds in this article. However, we cut off the high-frequency variations with a timescale of eight seconds according to our method to

obtain the RHESSI light curves. Thus, the rapidly varying component refers to variations with a timescale in the range of 8 – 240 seconds, while the slowly varying component refers to variations with a timescale longer than 240 seconds. The blue line shows the slowly varying component overlapping on the 3 – 6 keV light curve in the third panel, while the rapidly varying component is shown in the fourth panel. To study the oscillation in detail, wavelet analysis (*e.g.* De Moortel, Munday, and Hood, 2004; Delouille *et al.*, 2005) was used to analyze the rapidly varying component. Figure 1 (bottom panel) gives the wavelet analysis results, which clearly show a period of about two minutes around the 3 – 6 keV maximum, *i.e.* from 04:48 UT to 04:55 UT.

Imaging analysis can reveal the spatial structure of the flare sources that produces the oscillations. First, we produced CLEAN images in seven energy bands from 3 keV to 20 keV, *i.e.* 3 – 6 keV, 6 – 8 keV, 8 – 10 keV, 10 – 12 keV, 12 – 14 keV, 16 – 18 keV, and 18 – 20 keV, with an eight-second temporal resolution of the total flux light curve in Figure 1 (third and fourth panels), between 04:48 UT and 05:08 UT, which covers the 3 – 6 keV maximum completely. The image has a size of 64×64 pixels; each pixel is one arcsec across. We used the front detectors 3 to 8, excluding front detector 7. The images from 04:52:30 UT to 05:05:55 UT are shown in Figures 3, 4, and 5, but with a five-second cadence (shown in detail below). The contour levels are set at 56 %, 72 %, and 90 % of the local maximum in each image. Three green boxes are overplotted in the same way as in Figure 1. After integrating the flux in the three green boxes at different times, we obtained the light curves of each source from the flaring images (Figure 2 third panel). There are several peaks on the S_3 light curve, marked with pink vertical lines, but they are hardly visible on the light curves of S_1 and S_2.

To analyze the oscillations in the light curves of the three sources, we used the same Fourier analysis as before to decompose each source's light curve into a slowly varying component and a rapidly varying component, which are shown in Figure 6 (top and middle). The black lines show the source light curves, while the overplotted blue lines are the slowly varying component in the top panel, and the rapidly varying component is plotted in the middle panel. As in Figure 2, the rapidly varying component refers to variations with a timescale in the range of 8 – 240 seconds, the slowly varying component refers to variations with a timescale longer than 240 seconds. It is clear that the three rapidly varying components show a damped oscillation from 04:50 UT to 05:04 UT, which covers the flare maximum. In total, there are seven peaks on the three light curves, plotted with vertical pink lines, which occur at the same times as the vertical pink lines in Figure 2. Their mean period is about two minutes. S_1 oscillates with the same phase as S_3, but almost in anti-phase with S_2. The damped sine function $f = a_0 \exp(-t/\tau) \sin(2\pi t/a_1 + a_2)$ was used to fit the oscillation behavior, overplotted as the blue lines in Figure 6 (middle). The fitting parameters of $a \ni [a_0, a_1, a_2, \tau]$ are also given for each oscillation. The damped oscillation timescales are $\tau_{S_1} = 2.5$ minutes, $\tau_{S_2} = 6$ minutes, $\tau_{S_3} = 2.6$ minutes (between 04:50 – 04:56 UT), and $\tau_{S_3} = 4.3$ minutes (between 04:56 – 05:04 UT). It is interesting that S_3 shows an enhanced oscillation amplitude around 04:56 UT. Therefore, we fitted its oscillation behavior twice in the intervals between 04:50 – 04:56 UT (for A_p) and 04:56 – 05:04 UT (for A_f). The bottom panels show the wavelet analysis results of the rapidly varying component, which further confirm that all three sources display the oscillations with a two-minute period. All three sources show that the oscillation power is strong between 04:50 – 04:52 UT, which is before the flare maximum. S_3 shows an enhanced oscillation power around 04:58 UT, which is after the flare maximum.

It is known that there are several artifacts in RHESSI light curves that can be erroneously interpreted as quasi-periodic oscillations of solar flare X-ray emission. This problem was discussed by Inglis *et al.* (2011). One such artifact, which could be the most relevant to the

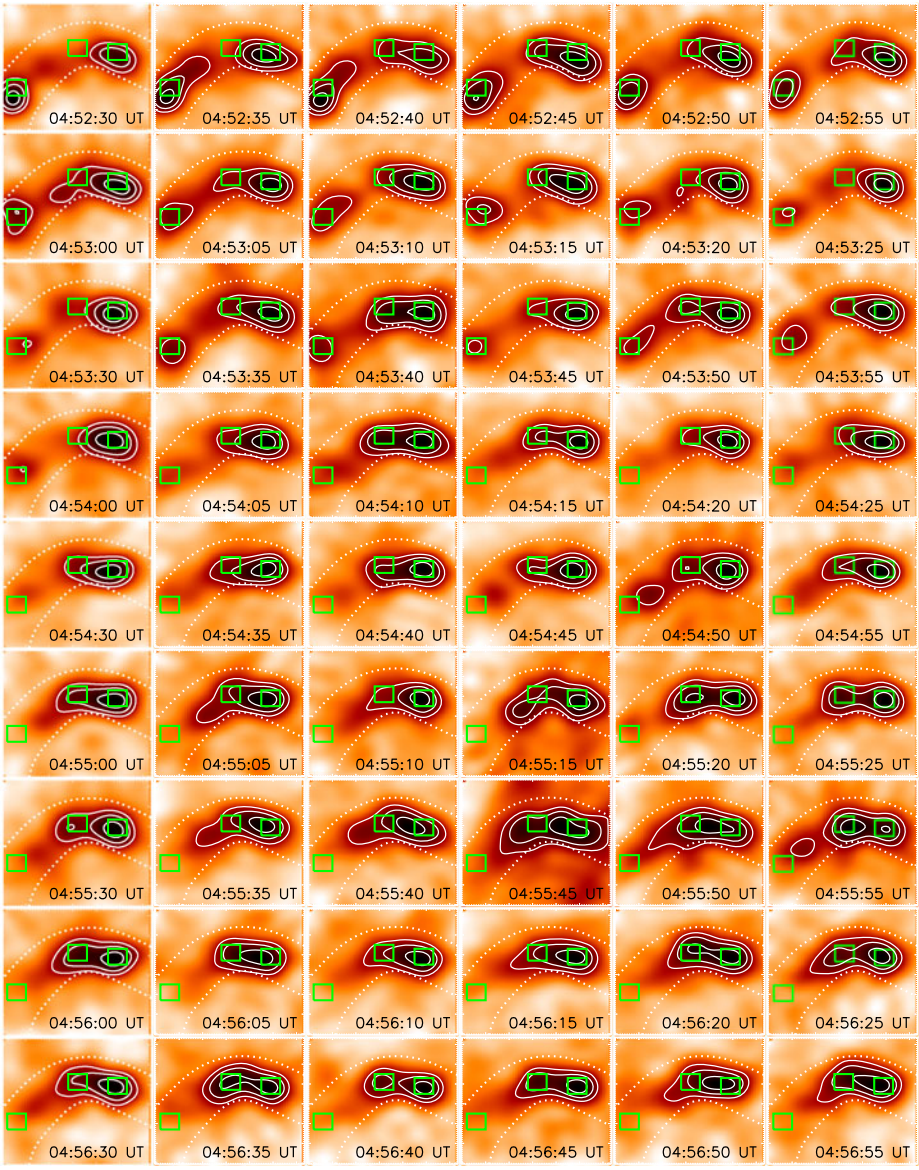

Figure 3 RHESSI CLEAN images at 3 – 6 keV with contours between 04:52:30 UT and 04:56:55 UT; the levels are set at 62 %, 76 %, and 90 % of the maximum. Each image has an integration time of eight seconds with a cadence of five seconds. The two dotted lines outline the flaring loop. Each image has a size of 64×64 arcsec^2. Front detectors 3 – 8 were used, excluding front detector 7.

observed two-minute oscillations here, is possibly due to nutation of the RHESSI spacecraft. However, the finding that S_2 oscillates almost in anti-phase to S_1 or S_3 rules this possibility out. It would be convincing if the two-minute oscillations found in the 3 – 6 keV RHESSI light curves here could be confirmed by another independent instrument on an other spacecraft in the future.

Figure 4 RHESSI CLEAN images at 3 – 6 keV with contours between 04:57:00 UT and 05:51:25 UT; the levels are set at 62 %, 76 %, and 90 % of the maximum. Each image has an integration time of eight seconds with a cadence of five seconds. The two dotted lines outline the flaring loop. Each image has a size of 64×64 arcsec^2. Front detectors 3 – 8 were used, excluding front detector 7.

2.2. Imaging Observations of Oscillation at 3 – 6 keV

Figure 1 shows that source S_3 is close to S_2, and both of them contribute to the flare X-ray emission. To study oscillation images with a high temporal resolution, we reconstructed RHESSI CLEAN images at 3 – 6 keV with an eight-second integration time and a one-

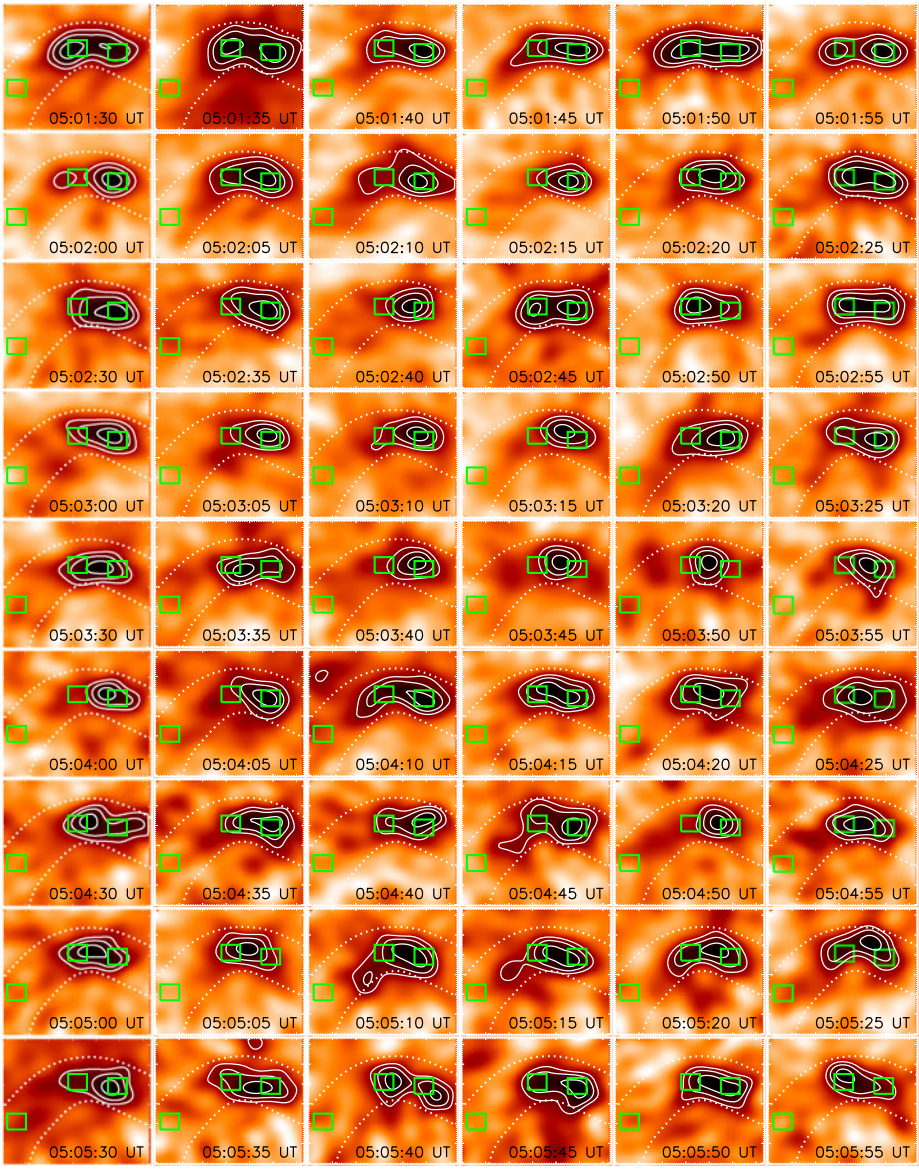

Figure 5 RHESSI CLEAN images at 3 – 6 keV with contours between 05:01:30 UT and 05:05:55 UT; the levels are set at 62 %, 76 %, and 90 % of the maximum. Each image has an integration time of eight seconds with a cadence of five seconds. The two dotted lines outline the flaring loop. Each image has a size of 64×64 arcsec^2. Front detectors 3 – 8 were used, excluding front detector 7.

second cadence between 04:48 UT and 05:08 UT. In other words, we used an eight-second integration window for each image and shifted it by one second, *i.e.* with seven seconds overlap between adjacent images. In this way, we obtained flare images with a high cadence of one second. Figure 3 to 5 show images with a five-second cadence. As in Figure 1, two dotted lines show the loop projection onto the solar disk, fully covering the 3 – 6 keV maximum

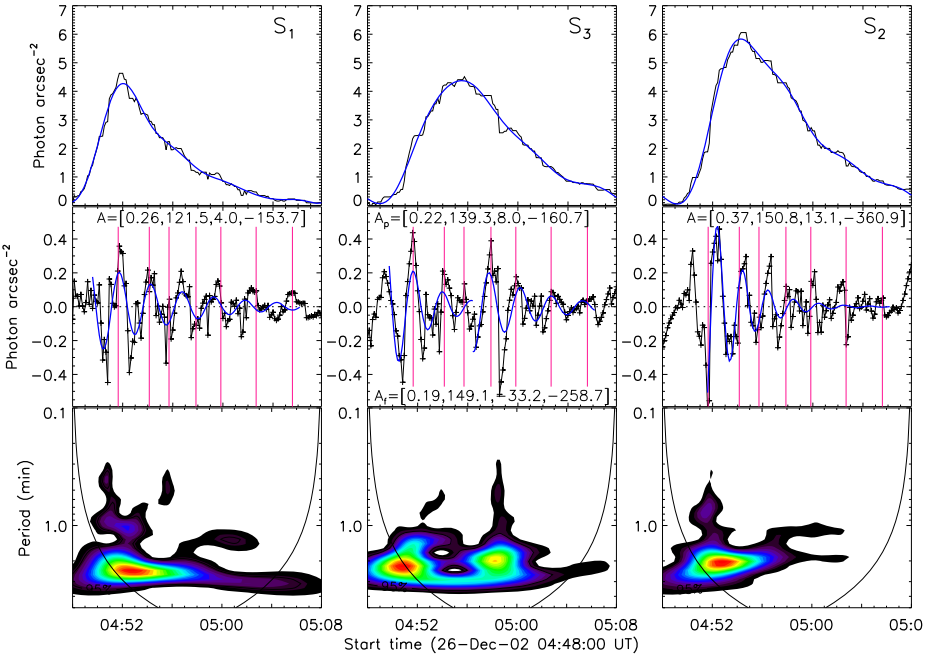

Figure 6 Top: temporal evolution of the S_1, S_2, and S_3 integration fluxes (black) with an eight-second temporal resolution; blue lines represent the slowly varying components. Middle: temporal evolution of the rapidly varying components; blue lines are sine-function fitting curves. The vertical pink lines indicate the seven peaks on the light curves that occur at the same times as the vertical pink lines in Figure 2. Bottom: wavelet spectra of the rapidly varying components.

brightness at various times. High-cadence images show that the S_3 sources are related to S_2 during the flare development. The position of S_2 is stable and always remains at the same location. However, S_3 does not always appear. For example, there are two sources of S_1 and S_2 at 04:54:00 UT in Figure 3, then S_2 broadens along the loop with a curved shape source after five seconds. At 04:54:10 UT, the flare shows three sources at the loop top and footpoints, which are recognized as S_1, S_2, and S_3 here, although S_1 is very weak. S_3 becomes faint at 04:54:15 UT, and the flare displays a curved source shape again five seconds later. Thus, there is a peak at 04:54:10 UT on S_3 light curve. In total, S_3 independently appears seven times with a period of two minutes, *i.e.* at 04:51:40 UT, 04:54:10 UT, 04:55:45 UT, 04:57:50 UT, 04:59:55 UT, 05:02:45 UT, and 05:05:40 UT, at which S_3 is clearly separated from S_2. These times correspond well to the seven peaks on the S_3 light curve marked with the pink vertical lines in Figure 2 (third panel) and Figures 6 and 7 (middle panel). At these times, the flare has three sources, two footpoint sources of S_1 and S_2, and a loop-top source of S_3 between them, which is the typical flare picture seen at X-rays. However, S_1 becomes gradually weaker after the flare maximum and cannot be seen during the decay phase.

Except for these seven times when S_3 separated from S_2 completely, there are additional separations or mergers of S_3 and S_2 into a curved source in the intervals between peaks. In other words, among these seven peaks, S_3 does not disappear absolutely, and there are additional subpeaks on the S_3 light curve. Sometimes, S_3 is also completely separated from S_2, sometimes, S_3 merges with S_2 into a curved shape source. For example, at 04:53:25 UT in Figure 3, there are two sources of S_1 and S_2 at 3 – 6 keV. The region of source S_3 is dim.

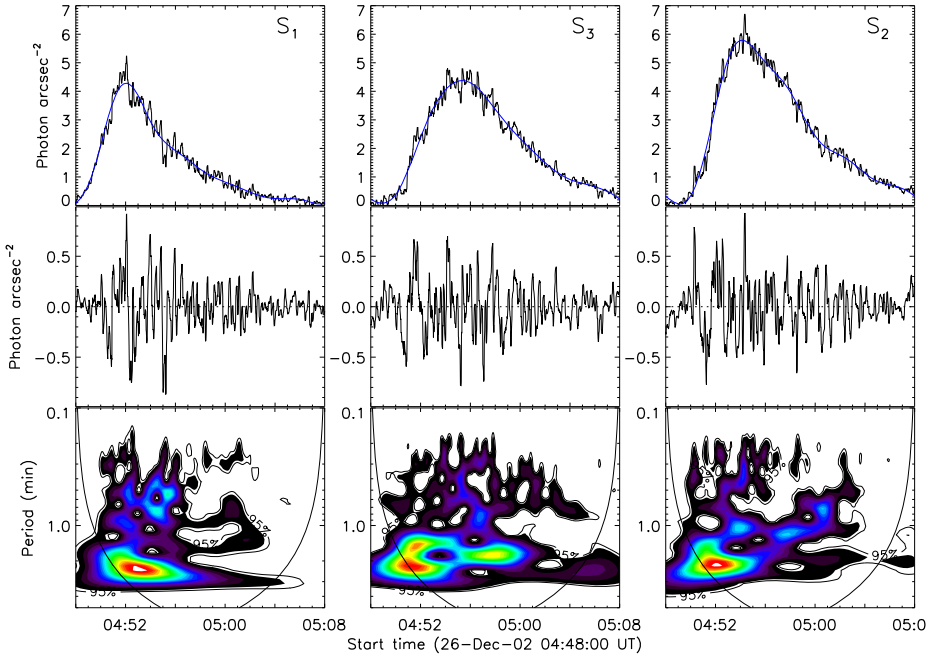

Figure 7 Top: temporal evolution of the S_1, S_2, and S_3 integration fluxes (black) with a one-second temporal resolution; blue lines represent the slowly varying components. Middle: temporal evolution of the rapidly varying components; blue lines are sine function fitting curves. The vertical pink lines mark the seven peaks on the light curves that occur at the same times as the vertical pink lines in Figure 2. Bottom: wavelet spectra of the rapidly varying components.

However, source S_2 gradually enlarges along the loop and reaches the loop top at 04:53:35 UT. After five seconds (at 04:53:40 UT), the 3 – 6 keV emission is bright along the flaring loop. The flare displays a curved source. The green box of S_3 also becomes brighter than before. Although S_3 is merged with S_2, there is an earlier subpeak just before 04:53:40 UT (marked in Figure 2) on the S_3 light curve. After that, this curved source starts to gradually become thin, and finally, *i.e.* at 04:53:45 UT, S_3 becomes very weak when the curved source shrinks and returns to the original position of S_2 at 04:53:25 UT. Five seconds later, S_3 appears again and separately from S_2 at 04:53:50 UT, but there is no subpeak at this time, which is also marked with a black vertical line in Figure 2. At 04:53:45 UT, the image shows that the curved source shrinks back to S_2. In total, these features appear 26 times between 04:50 UT and 05:08 UT, indicated by the black vertical lines in Figure 2. Sometimes, there are subpeaks corresponding to these features, *e.g.* at 04:52:40 UT and 05:01:50 UT and later, but sometimes there are no subpeaks, *e.g.* at 04:57:40 UT on the S_3 light curve. Figures 3 to 5 show the images of these 26 times from 04:51:40 UT to 05:05:40 UT. The average period of these vertical lines is about 25 seconds.

As noted earlier, three green boxes are used to identify the three source regions. After integrating the fluxes of the three boxes in each image, Figure 7 (top) plots the light curves of S_1, S_2, and S_3 with a rapid cadence of one second. According to our method, only every eighth point is independent in these light curves. Using the Fourier analysis as before, three light curves were decomposed into the rapidly varying and slowly varying components. Here the rapidly varying component refers to variations with a timescale in the range

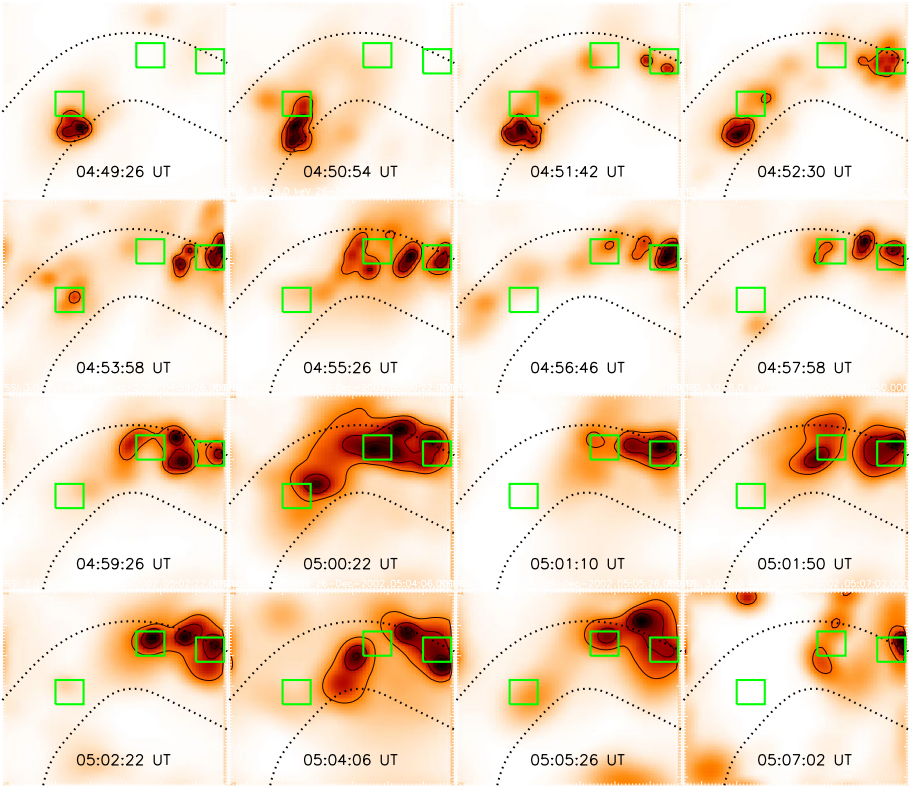

Figure 8 RHESSI PIXON at 3 – 6 keV with contours between 04:49:26 UT and 05:07:02 UT; the contour levels are set at 30 %, 55 %, and 80 % of the maximum. Each image has a size of 64 × 64 arcsec^2 and an integration time of eight seconds; all detectors are used. The two dotted lines outline the flaring loop.

of 1 – 240 seconds, and the slowly varying component refers to variations with a timescale longer than 240 seconds. The wavelet analysis results of the rapidly varying components are plotted in the bottom, which again confirms the two-minute oscillation in three sources. The results show the fast oscillations from the light curves of three sources; specifically, S_2 displays a 25-second oscillation from 04:52 UT to 04:54 UT, while S_3 displays an oscillations with a wide period range of shorter than 60 seconds.

In addition to the RHESSI CLEAN images in Figures 3 to 5, RHESSI PIXON images are also shown in Figure 8 between 04:49:26 UT and 05:07:02 UT. PIXON allows us to investigate the morphology of the sources and their dynamics in more detail. These images were reconstructed with an integration of an eight-second time and all front detectors. Thus, the spatial resolution of these images reaches up to 2.3 arcsec. As shown in Figures 3 to 5 with the CLEAN algorithm, the 26 December 2002 flare region consists of three X-ray sources marked by S_1, S_2, and S_3. However, the structure of the X-ray sources in the flare region is much more complex in the PIXON images. For example, there are two sources, S_2 and S_3, at 04:55:25 UT in Figure 3, but three sources at 04:55:26 UT in Figure 8. There is another apparent source between S_2 and S_3 in the PIXON image. Here, Figure 8 only displays the flare images at the times of the dips and peaks of the rapidly varying component

of S_3 in Figure 6. However, the three green boxes still roughly mark the bulk of the X-ray emission at 3 – 6 keV in Figure 8.

3. Conclusions

We have analyzed the quasi-periodic oscillations at X-ray emission as low as 3 – 6 keV in the 26 December 2002 flare observed by RHESSI. Although only few similarly detailed observations have been reported in the literature, this article presented three important features: i) the low X-ray class of the observed flare, *i.e.* B8.1; ii) the low energies of X-ray emission at which the quasi-periodic oscillations are found, *i.e.* lower than about 6 keV; iii) an attempt to reveal spatial structure of the flare sources that produce the oscillations.

The 26 December 2002 flare displays several peaks on the light curve at 3 – 6 keV, but shows smooth light curves at 6 – 12 keV and 12 – 25 keV. The detailed analysis with Fourier and wavelet methods showed that these peaks oscillate with an average period of about two minutes. RHESSI gives us the opportunity to study the images of quasi-periodic oscillations with a high temporal resolution. First, we reconstructed the CLEAN images in seven energy bands from 3 keV to 20 keV, with an eight-second integration window. The flare images showed the two footpoint sources of S_1 and S_2 and a loop-top source of S_3, whose positions are consistent with the MDI magnetogram and EIT 195 Å observations. Second, the flare loop shape was outlined based on the X-ray source positions at different times and at various energy bands. Three sources, S_1, S_2, and S_3 are located in this artificial loop. After integrating the fluxes at each source region, we obtained for each source light curves that displayed seven peaks overlapped on the background emissions. From the image observations, we found that each peak was consistent with the time when S_3 was split from S_2 completely. Third, each light curve was decomposed into the rapidly varying and slowly varying (background) components using the Fourier method. The rapidly varying components of three sources displayed a damped oscillation with a period of two minutes. S_3 showed a complicated oscillation behavior. It was triggered twice, at the flare onset and after the maximum. The damped oscillation timescale had a duration of between 2.5 – 6 minutes. S_2 displayed stronger damping than S_1 and S_3. S_1 oscillated at the same phase as S_3, but almost in antiphase with S_2. Finally, we produced CLEAN images with an eight-second integration and a one-second cadence. Using Fourier and wavelet method, each source light curve with a rapid cadence of one second was analyzed; the results confirmed the two-minute oscillation in three sources. However, there were other fast periodic oscillations corresponding to the subpeaks on their light curves, *i.e.* periods shorter than one minute were also detected, especially the 25-second oscillation in S_2 and S_3. Imaging observations show that these oscillation subpeaks appeared at the time when S_3 merged with S_2 into a curved-shape source, while at other times S_3 became faint and was hardly visible.

Figure 9 shows the RHESSI spectra around the flare maximum of the 26 December 2002 flare, indicating that the 3 – 6 keV emission belongs to the thermal component and that the two-minute oscillation at 3 – 6 keV is due to a quasi-periodic heating mechanism. This might be caused by the quasi-periodic electron acceleration from the magnetic reconnection. According to the flare model, the footpoint sources are generally produced by the accelerated electrons via electron–ion bremsstrahlung as they lose their energy and heat the local atmosphere. Therefore, the quasi-periodic reconnection results in electron acceleration, which in turn causes the quasi-periodic heating. The indicated evidence of quasi-periodic reconnection has been reported in solar flares (*e.g.* Nakajima *et al.*, 1983; Asai *et al.*, 2001; Ning *et al.*, 2005; Li and Gan, 2008). However, for the 26 December 2002 flare, one of the

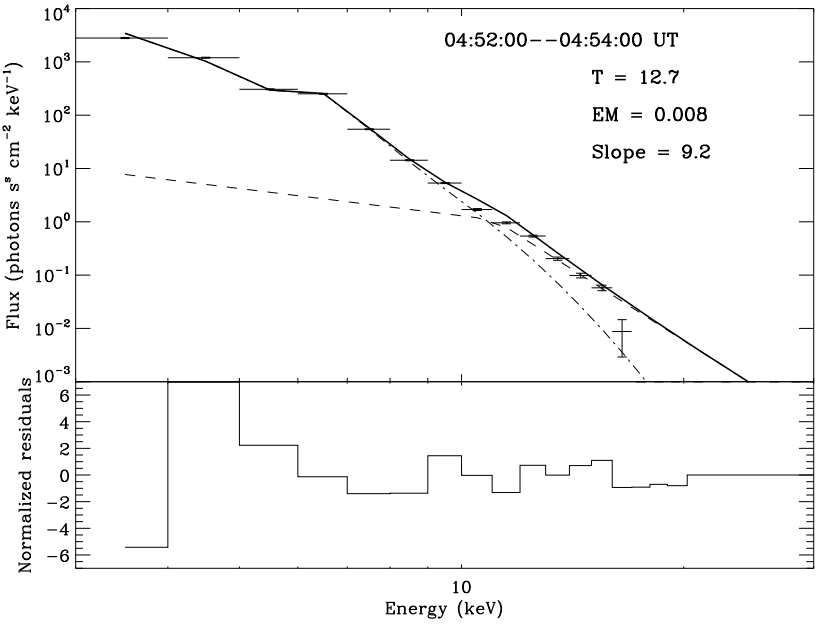

Figure 9 Upper panel: RHESSI spectra between 04:52 and 04:54 UT around the maximum of the 26 December 2002 flare. The points with error bars represent the observational data. Different lines show the model spectral fits for the thermal component (dot-dashed line), nonthermal broken power-law shape (dashed line), and a summation of the two (thick solid line). The fitting parameters of temperature [T in units of MK], emission measure [EM in units of 10^{49} cm^{-3}], and power-law slope are given. Bottom panel: Normalized residuals in the energy range between 3 and 20 keV for spectral fitting.

footpoint sources of S_1 displays a two-minute oscillation almost in anti-phase to the other footpoint of S_2, which seems to contradict the heating from quasi-periodic reconnection. If quasi-periodic heating were due to the thermalization of populations of nonthermal electrons accelerated quasi-periodically in the reconnection region, this would also be accompanied by quasi-periodic pulsations of nonthermal HXR emission. This is not observed, however.

4. Discussion

Explaining the period of the S_3 source is an interesting challenge. According to the flare topology in Figure 1, the source of S_3 is a loop top, while S_1 and S_2 are two footpoint sources. As noted earlier, we plotted the flare loop with the dashed lines in Figures 1 to 5. S_3 displays a mean period of two minutes, and the maximum distance between S_3 and S_2 is about 20 arcsec. The velocity of S_3 is roughly 130 km s^{-1} (the maximum distance of the S_3 movement is about 20 arcsec, and S_3 appears with a period of two minutes), which is slightly slower than the sound speed ($c_s = 0.166\sqrt{T} \approx 600$ km s^{-1}; here the temperature [T] is 12.7 MK in Figure 9) or the evaporation speed (around 400 km s^{-1}) found in solar flares (Aschwanden and Benz, 1995; Czaykowska *et al.*, 1999; Ji *et al.* 2004, 2006, 2008; Milligan *et al.*, 2006; Shen *et al.*, 2008; Brosius and Holman, 2007; Ning *et al.*, 2009; Milligan and Dennis, 2009; Ning and Cao 2010a, 2010b, 2011; Ning, 2011). It is reminiscent of the chromospheric evaporation contribution to the source S_3 appearance with

a two-minute period. In this case, the quasi-periodic reconnection has driven the quasi-periodic acceleration, followed by quasi-periodic evaporation. According to this scenario, the footpoint source of S_2 should disappear at 3 – 6 keV, while only the high-energy source remains when the loop-top source S_3 appears after the evaporation (Ning *et al.*, 2009; Ning, 2011), which is not consistent with our observation, indicating that the evaporation scenario is not responsible for the appearance of S_3. That source S_3 appeared separately from source S_2 during the peak of the two-minute oscillations may be due to the restricted dynamic range of the RHESSI telescope ($\approx$ ten). It is possible that during the peaks of the oscillations the intensity of source S_3 is quite high and similar to (within a factor of ten) the intensity of source S_2, hence at these times RHESSI can see source S_3 as distinct from source S_2. In contrast, during the oscillation gaps, the intensity of source S_3 is much lower than of source S_2, and the dynamic range of RHESSI is not sufficient to separate source S_3 from the more intense source S_2, and source S_3 seems to merge with source S_2.

Another possibility is that source S_3 is not a loop-top source, but a third footpoint source similar to S_1 and S_2. Figure 1 shows that there is a positive magnetic field at the edge of the negative field, and S_2 tends to occur in the negative region, while S_3 tends to occur in the positive region. In this case, there should be two loop systems in this flare; the larger one (about 66 arcsecs long according to the dashed lines in Figures 1 to 5) connecting S_1 and S_2, the smaller one (about 20 arcsecs long) connecting S_2 and S_3. Our observations show that source S_1 oscillates with the same phase as S_3, but is almost in anti-phase with S_2. These connections suggest that S_1 and S_2, and S_2 and S_3 are two conjugated footpoints. In this scenario, the quasi-periodic reconnection can drive the quasi-periodic oscillation at S_1 and S_2 in the same phase, but fails to explain the quasi-periodic oscillations at S_2 and S_3 in the anti-phase, which indicates wave model oscillations in this small loop, probably MHD waves, but not an Alfvén wave. Because an Alfvén wave has a speed of 40 000 km s^{-1} (we estimated it with the observational parameters, such as a 1000 Gauss field, EM in Figure 9, and 20-arcsec source length to derive the flare volume), which is much larger than the S_3 source speed of 130 km s^{-1}. In other words, the quasi-periodic reconnection produces the quasi-periodic oscillation at S_1 and S_2 and drives the quasi-periodic MHD waves at S_2. These waves propagate toward the footpoint S_3, which displays the oscillation in anti-phase, but with the same period as S_2. In contrast, sources S_1 and S_3, and sources S_3 and S_2 are conjugate footpoints of two different loop-systems: S_1–S_3 and S_3–S_2. In this case the same phase oscillations in S_1 and S_3 could be explained by simultaneous heating of the S_1–S_3 loop system, while the anti-phase oscillations in S_3 and S_2 (as well as in S_1 and S_2) are due to the time delay required by the heat flow to bridge the gap between S_3 and S_2 along the loop-system S_3–S_2.

We found that the 26 December 2002 flare displays two-minute oscillations. From an imaging analysis of the flare region, we also found that the oscillations originate from separated sources in anti-phase. The situation in the small (B8.1) flare is reminiscent of the situation in the much more powerful M1.8 flare discussed by Zimovets and Struminsky (2010). We also found that the quasi-periodic oscillations (with a period of 16 seconds) of the SXR and HXR emission have their origin in two spatially separated, but interacting systems of flaring loops of the same active region. The physical mechanism that is responsible for the quasi-periodic energy release in both flares is probably the same. The source region of S_2 possibly belongs to a different loop system from S_1 and S_3. Their oscillations are excited by the same quasi-periodic energy release process. Different flaring loop systems display a similar oscillation behavior, but different oscillation phases due to a spatially separated origin. RHESSI PIXON images show that S_2 is spatially more clearly separated from S_3 than it is in the CLEAN images.

Acknowledgements We would like to thank the anonymous referee for their valuable comments that improved this article. The data used here are taken from RHESSI, SOHO/MDI and SOHO/EIT. This work is supported by NSF of China under grants 11173063, 10833007, 10973042, 973 Program under grant 2011CB811402 and Laboratory No. 2010DP173032.

References

Asai, A., Shimojo, M., Isobe, H., Morimoto, T., Yokoyama, T., Shibasaki, K., Nakajima, H.: 2001, *Astrophys. J. Lett.* **562**, L103. ADS:2001ApJ...562L.103A. doi:10.1086/338052.

Aschwanden, M.J., Benz, A.O.: 1995, *Astrophys. J.* **438**, 997. ADS:1995ApJ...438..997A. doi:10.1086/175141.

Aschwanden, M.J., Benz, A.O., Montello, M.L.: 1994, *Astrophys. J.* **431**, 432. ADS:1994ApJ...431..432A. doi:10.1086/174497.

Aschwanden, M.J., Benz, A.O., Dennis, B.R., Schwartz, R.A.: 1995, *Astrophys. J.* **455**, 347. ADS:1995ApJ...455..347A. doi:10.1086/176582.

Aschwanden, M.J., Bynum, R.M., Kosugi, T., Hudson, H.S., Schwartz, R.A.: 1997, *Astrophys. J.* **487**, 936. ADS:1997ApJ...487..936A. doi:10.1086/304633.

Aschwanden, M.J., Kliem, B., Schwarz, U., Kurths, J., Dennis, B.R., Schwartz, R.A.: 1998, *Astrophys. J.* **505**, 941. ADS:1998ApJ...505..941A. doi:10.1086/306200.

Bogovalov, S.V., Iyudin, A.F., Kotov, Y.D., Dolidze, V.I., Estulin, I.V., Vedrenne, G., Niel, M., Barat, C., Chambon, G., Talon, M.: 1983, *Sov. Astron. Lett.* **9**, 163. ADS:1983SvAL....9..163B.

Bogovalov, S.V., Iyudin, A.F., Kotov, Y.D., Shugal, E.V., Dolidze, V.S., Zenchenko, V.M., Vedrenne, G., Niel, M., Barat, C., Chambon, G., Talon, R.: 1984, *Sov. Astron. Lett.* **10**, 286. ADS:1984SvAL...10..286B.

Brosius, J.W., Holman, G.D.: 2007, *Astrophys. J. Lett.* **659**, L73. ADS:2007ApJ...659L..73B. doi:10.1086/516629.

Czaykowska, A., de Pontieu, B., Alexander, D., Rank, G.: 1999, *Astrophys. J. Lett.* **521**, L75. ADS:1999ApJ...521L..75C. doi:10.1086/312176.

De Moortel, I., Munday, S.A., Hood, A.W.: 2004, *Solar Phys.* **222**, 203. ADS:2004SoPh..222..203D. doi:10.1023/B:SOLA.0000043578.01201.2d.

De Moortel, I., Ireland, J., Hood, A.W., Walsh, R.W.: 2002, *Astron. Astrophys. Lett.* **387**, L13. ADS:2002A& A...387L..13D. doi:10.1051/0004-6361:20020436.

Delaboudinière, J.-P., Artzner, G.E., Brunaud, J., Gabriel, A.H., Hochedez, J.F., Millier, F., Song, X.Y., Au, B., Dere, K.P., Howard, R.A., Kreplin, R., Michels, D.J., Moses, J.D., Defise, J.M., Jamar, C., Rochus, P., Chauvineau, J.P., Marioge, J.P., Catura, R.C., Lemen, J.R., Shing, L., Stern, R.A., Gurman, J.B., Neupert, W.M., Maucherat, A., Clette, F., Cugnon, P., van Dessel, E.L.: 1995, *Solar Phys.* **162**, 291. ADS:1995SoPh..162..291D. doi:10.1007/BF00733432.

Delouille, V., de Patoul, J., Hochedez, J.F., Jacques, L., Antoine, J.P.: 2005, *Solar Phys.* **228**, 301. ADS:2005SoPh..228..301D. doi:10.1007/s11207-005-5620-3.

Dmitriev, P.B., Kudryavtsev, I.V., Lazutkov, V.P., Matveev, G.A., Savchenko, M.I., Skorodumov, D.V., Charikov, Y.E.: 2006, *Solar Syst. Res.* **40**, 142. ADS:2006SoSyR..40..142D. doi:10.1134/S0038094606020080.

Domingo, V., Fleck, B., Poland, A.I.: 1995, *Solar Phys.* **162**, 1. ADS:1995SoPh..162....1D. doi:10.1007/BF00733425.

Foullon, C., Verwichte, E., Nakariakov, V.M., Fletcher, L.: 2005, *Astron. Astrophys. Lett.* **440**, L59. ADS:2005A& A...440L..59F. doi:10.1051/0004-6361:200500169.

Harrison, R.A.: 1987, *Astron. Astrophys.* **182**, 337. ADS:1987A& A...182..337H.

Hoyng, P., van Beek, H.F., Brown, J.C.: 1976, *Solar Phys.* **48**, 197. ADS:1976SoPh...48..197H. doi:10.1007/BF00151992.

Inglis, A.R., Zimovets, I.V., Dennis, B.R., Kontar, E.P., Nakariakov, V.M., Struminsky, A.B., Tolbert, A.K.: 2011, *Astron. Astrophys.* **530**, A47. ADS:2011A& A...530A..47I. doi:10.1051/0004-6361/201016322.

Isliker, H., Benz, A.O.: 1994, *Astron. Astrophys. Suppl. Ser.* **104**, 145. ADS:1994A& AS..104..145I.

Ji, H., Wang, H., Goode, P.R., Jiang, Y., Yurchyshyn, V.: 2004, *Astrophys. J. Lett.* **607**, L55. ADS:2004ApJ...607L..55J. doi:10.1086/421550.

Ji, H., Huang, G., Wang, H., Zhou, T., Li, Y., Zhang, Y., Song, M.: 2006, *Astrophys. J. Lett.* **636**, L173. ADS:2006ApJ...636L.173J. doi:10.1086/500203.

Ji, H., Wang, H., Liu, C., Dennis, B.R.: 2008, *Astrophys. J.* **680**, 734. ADS:2008ApJ...680..734J. doi:10.1086/587138.

Jin, M., Ding, M.D.: 2007, *Astron. Astrophys.* **471**, 705. ADS:2007A& A...471..705J. doi:10.1051/0004-6361:20077202.

Kliem, B., Karlický, M., Benz, A.O.: 2000, *Astron. Astrophys.* **360**, 715. ADS:2000A& A...360..715K.
Kliem, B., Dammasch, I.E., Curdt, W., Wilhelm, K.: 2002, *Astrophys. J. Lett.* **568**, L61. ADS: 2002ApJ...568L..61K. doi:10.1086/340136.
Kupriyanova, E.G., Melnikov, V.F., Nakariakov, V.M., Shibasaki, K.: 2010, *Solar Phys.* **267**, 329. ADS:2010SoPh..267..329K. doi:10.1007/s11207-010-9642-0.
Li, Y.P., Gan, W.Q.: 2008, *Solar Phys.* **247**, 77. ADS:2008SoPh..247...77L. doi:10.1007/s11207-007-9092-5.
Lin, R.P., Dennis, B.R., Hurford, G.J., Smith, D.M., Zehnder, A., Harvey, P.R., *et al.*: 2002, *Solar Phys.* **210**, 3. ADS:2002SoPh..210....3L. doi:10.1023/A:1022428818870.
Lipa, B.: 1978, *Solar Phys.* **57**, 191. ADS:1978SoPh...57..191L. doi:10.1007/BF00152054.
Mangeney, A., Pick, M.: 1989, *Astron. Astrophys.* **224**, 242. ADS:1989A& A...224..242M.
Masuda, S., Kosugi, T., Hara, H., Tsuneta, S., Ogawara, Y.: 1994, *Nature* **371**, 495. ADS: 1994Natur. 371..495M. doi:10.1038/371495a0.
McKenzie, D.E., Mullan, D.J.: 1997, *Solar Phys.* **176**, 127. ADS:1997SoPh..176..127M. doi:10.1023/A:1004984125700.
Melnikov, V.F., Reznikova, V.E., Shibasaki, K., Nakariakov, V.M.: 2005, *Astron. Astrophys.* **439**, 727. ADS:2005A& A...439..727M. doi:10.1051/0004-6361:20052774.
Milligan, R.O., Dennis, B.R.: 2009, *Astrophys. J.* **699**, 968. ADS:2009ApJ...699..968M. doi:10.1088/0004-637X/699/2/968.
Milligan, R.O., Gallagher, P.T., Mathioudakis, M., Bloomfield, D.S., Keenan, F.P., Schwartz, R.A.: 2006, *Astrophys. J. Lett.* **638**, L117. ADS:2006ApJ...638L.117M. doi:10.1086/500555.
Nakajima, H., Kosugi, T., Kai, K., Enome, S.: 1983, *Nature* **305**, 292. ADS:1983Natur. 305..292N. doi:10.1038/305292a0.
Nakariakov, V.M.: 2007 In: *AGU Spring Meeting Abs.*, A6. ADS:2007AGUSMSH22A..06N.
Nakariakov, V.M., Melnikov, V.F.: 2009, *Space Sci. Rev.* **149**, 119. ADS:2009SSRv..149..119N. doi:10.1007/s11214-009-9536-3.
Nakariakov, V.M., Ofman, L., DeLuca, E.E., Roberts, B., Davila, J.M.: 1999, *Science* **285**, 862. ADS:1999Sci...285..862N. doi:10.1126/science.285.5429.862.
Nakariakov, V.M., Foullon, C., Verwichte, E., Young, N.P.: 2006, *Astron. Astrophys.* **452**, 343. ADS:2006A& A...452..343N. doi:10.1051/0004-6361:20054608.
Nakariakov, V.M., Foullon, C., Myagkova, I.N., Inglis, A.R.: 2010, *Astrophys. J.* **708**, L47. ADS: 1999Sci...285..862N. doi:10.1126/science.285.5429.862.
Ning, Z.: 2011, *Solar Phys.* **273**, 81. ADS:2011SoPh..273...81N. doi:10.1007/s11207-011-9833-3.
Ning, Z., Cao, W.: 2010a, *Astrophys. J.* **717**, 1232. ADS:2010ApJ...717.1232N. doi:10.1088/0004-637X/717/2/1232.
Ning, Z., Cao, W.: 2010b, *Solar Phys.* **264**, 329. ADS:2010SoPh..264..329N. doi:10.1007/s11207-010-9589-1.
Ning, Z., Cao, W.: 2011, *Solar Phys.* **269**, 283. ADS:2011SoPh..269..283N. doi:10.1007/s11207-010-9693-2.
Ning, Z., Ding, M.D., Wu, H.A., Xu, F.Y., Meng, X.: 2005, *Astron. Astrophys.* **437**, 691. ADS: 2005A& A...437..691N. doi:10.1051/0004-6361:20041944.
Ning, Z., Wu, H., Xu, F., Meng, X.: 2007, *Solar Phys.* **242**, 101. ADS:2007SoPh..242..101N. doi:10.1007/s11207-007-0412-6.
Ning, Z., Cao, W., Huang, J., Huang, G., Yan, Y., Feng, H.: 2009, *Astrophys. J.* **699**, 15. ADS: 2009ApJ...699...15N. doi:10.1088/0004-637X/699/1/15.
Ofman, L., Sui, L.: 2006, *Astrophys. J. Lett.* **644**, L149. ADS:2006ApJ...644L.149O. doi:10.1086/505622.
Ofman, L., Wang, T.: 2002, *Astrophys. J. Lett.* **580**, L85. ADS:2002ApJ...580..850S. doi:10.1086/343788.
Scherrer, P.H., Bogart, R.S., Bush, R.I., Hoeksema, J.T., Kosovichev, A.G., Schou, J., Rosenberg, W., Springer, L., Tarbell, T.D., Title, A., Wolfson, C.J., Zayer, I. (MDI Engineering Team): 1995, *Solar Phys.* **162**, 129. ADS:1995SoPh..162..129S. doi:10.1007/BF00733429.
Shen, J., Zhou, T., Ji, H., Wang, N., Cao, W., Wang, H.: 2008, *Astrophys. J. Lett.* **686**, L37. ADS:2008ApJ...686L..37S. doi:10.1086/592835.
Su, J.T., Shen, Y.D., Liu, Y.: 2012, *Astrophys. J.* **754**, 43. ADS:2012ApJ...754...43S. doi:10.1088/0004-637X/754/1/43.
Su, J.T., Shen, Y.D., Liu, Y., Liu, Y., Mao, X.J.: 2012, *Astrophys. J.* **755**, 113. ADS:2012ApJ...755..113S. doi:10.1088/0004-637X/755/2/113.
Svestka, Z., Dennis, B.R., Woodgate, B.E., Pick, M., Raoult, A., Rapley, C.G., Stewart, R.T.: 1982, *Solar Phys.* **80**, 143. ADS:1982SoPh...80..143S. doi:10.1007/BF00153429.
Sych, R., Nakariakov, V.M., Karlicky, M., Anfinogentov, S.: 2009, *Astron. Astrophys.* **505**, 791. ADS:2009A& A...505..791S. doi:10.1051/0004-6361/200912132.
Tan, B., Zhang, Y., Tan, C., Liu, Y.: 2010, *Astrophys. J.* **723**, 25. ADS:2010ApJ...723...25T. doi:10.1088/0004-637X/723/1/25.

Wang, T., Solanki, S.K., Curdt, W., Innes, D.E., Dammasch, I.E.: 2002, *Astrophys. J. Lett.* **574**, L101. ADS:2002ApJ...574L.101W. doi:10.1086/342189.

Wang, T.J., Solanki, S.K., Curdt, W., Innes, D.E., Dammasch, I.E., Kliem, B.: 2003, *Astron. Astrophys.* **406**, 1105. ADS:2003A& A...406.1105W. doi:10.1051/0004-6361:20030858.

Zhao, R.-Y., Mangeney, A., Pick, M.: 1991, *Astron. Astrophys.* **241**, 183. ADS:1991A& A...241..183Z.

Zimovets, I.V., Struminsky, A.B.: 2009, *Solar Phys.* **258**, 69. ADS:2009SoPh..258...69Z. doi:10.1007/s11207-009-9394-x.

Zimovets, I.V., Struminsky, A.B.: 2010, *Solar Phys.* **263**, 163. ADS:2010SoPh..263..163Z. doi:10.1007/s11207-010-9518-3.